

# Grain boundary excess free volume—direct thermodynamic measurement

L. S. Shvindlerman · G. Gottstein · V. A. Ivanov ·  
D. A. Molodov · D. Kolesnikov · W. Łojkowski

Received: 23 March 2006 / Accepted: 13 June 2006 / Published online: 2 November 2006  
© Springer Science+Business Media, LLC 2006

**Abstract** The grain boundary excess free volume (BFV) along with the surface tension determines the major thermodynamic properties of grain boundaries. The BFV controls to a large extent the evolution and stability of polycrystals. Unfortunately, our knowledge about the BFV is completely restricted to data generated by computer simulations, which, in turn, are strictly limited to grain boundaries in the vicinity of special misorientations. We developed a special technique that makes it possible to measure the BFV for practically any grain boundary and provides a way of estimating the BFV for grain boundaries of different classes with high accuracy. A knowledge of the BFV is especially important for fine grained and nanocrystalline systems where it opens new possibilities to design the physical properties and microstructure of such polycrystals.

## Introduction

The grain boundary excess free volume (BFV) is one of fundamental thermodynamic parameters of interfaces. Whereas the derivative  $\left(\frac{\partial \gamma}{\partial T}\right)_p$  ( $\gamma$ -interface

free energy) reflects the reaction of the interface on a temperature change, the derivative  $\left(\frac{\partial \gamma}{\partial p}\right)_T$  describes the reaction to the applied external pressure. Since the BFV defines conceptually the difference how the atoms are packed in the bulk and in the grain boundary, it determines the grain boundary diffusivity, the mobility, and to a certain extent, grain growth inhibition by vacancy generation. As a consequence, it affects the stability and the kinetics of grain growth of polycrystals under high pressures. The value of the BFV determines the driving force to “squeeze” a grain boundary out of a polycrystal. On the other hand the BFV influences grain growth and other process connected to the generation of vacancies [1–4]. This effect is especially pronounced in fine grained and nanocrystalline materials, or in thin films on a substrate where the BFV enforces an “equilibrium grain size” beyond which no grain growth occurs [2]. Unfortunately, up to now we are forced be content with the results of computer simulations, which, in turn, are strictly limited to grain boundaries in the vicinity of special misorientations [5–9]. Correlations between the BFV and grain boundary properties were discovered by Knizhnik [5], Wolf (energy) [6, 7], Zhang and Srolovitz (mobility) [10]. It was shown that similar to grain boundary mobility and diffusivity, the BFV misorientation dependence changes non-monotonically and assumes cusps for low  $\Sigma$  orientation relationships. Some experimental attempts were undertaken to determine the BFV [11,12]. Meiser and Gleiter [11] measured the change of misorientation for grain boundary energy cusps by applying a hydrostatic pressure of  $7 \times 10^8$  Pa. Merkle et al. [12] measured the BFV by HRTEM observations of the lattice parameter change in the vicinity of the interface between two

L. S. Shvindlerman  
Institute of Solid State Physics, Russian Academy of  
Sciences, Chernogolovka, Moscow District 142432, Russia

G. Gottstein (✉) · V. A. Ivanov · D. A. Molodov  
Institut für Metallkunde und Metallphysik, RWTH Aachen,  
Kopernikusstr. 14, Aachen D-52056, Germany  
e-mail: gottstein@imm.rwth-aachen.de

D. Kolesnikov · W. Łojkowski  
Institute of High Pressure Physics, Polish Academy of  
Sciences, Sokolowska 29, Warsaw 01-142, Poland

grains. The value of the BFV averaged over all different types of studies is in the range of  $10^{-12}$ – $10^{-10}$  m<sup>3</sup>/m<sup>2</sup>. It is stressed, however, that all estimates are based on models, since they have to rely on assumptions of the grain boundary width, which is unknown.

However, there is a correct thermodynamic way to determine the BFV at least for grain boundaries [13, 14]. Let us consider the Gibbs equation for the adsorption at interfaces

$$d\gamma = -s^s dT - \sum_{i=1}^k \Gamma_i d\mu_i + v^s dp \quad (1)$$

where  $s^s$  and  $v^s$  are the entropy and the volume of the surface,  $\Gamma_i$  and  $\mu_i$  are the adsorption and chemical potential of the  $i$ th component,  $T$  is the temperature.

In the Gibbs method, in a local sense,  $v^s = 0$  and Eq. 1 assumes the form

$$d\gamma = -s^s dT - \sum_{i=1}^k \Gamma_i d\mu_i \quad (2)$$

There is no sense in considering such a problem for an interphase, inasmuch as at constant temperature such a system is completely determined. A grain boundary separates two thermodynamically identical phases and one peculiarity of grain boundaries consists of the fact that for the system with a grain boundary the number of degrees of freedom is by one greater than for an interphase [13]. Therefore, for a system with a grain boundary all differentials on the right-hand side of Eq. 2 are independent; for a grain boundary the Gibbs–Duhem equation does not impose any restriction on the system. The surface excesses of the grain boundaries are independent of the position of the dividing surface and depend on the properties of the grain boundary only [13]. Due to the additional degree of freedom a number of unique possibilities arises. In particular, one can consider adsorption in a one-component system, which we shall call autoadsorption. Indeed, in this case Eq. 2 takes the form

$$d\gamma = -s^s dT - \Gamma_0 d\mu \quad (3)$$

The parameter  $\Gamma_0$  has the meaning of an autoadsorption at grain boundaries in a pure material. Expressing  $\mu$  through the thermodynamic characteristics of the volume of the grain and taking into account that  $s^s = \Gamma_0 s_a^s$ , where  $s_a^s$  is the surface excess of the entropy per atom at the surface (boundary) we arrive at [13].

$$d\gamma = -\Gamma_0 (s_a^s - s_a^v) dT - \Gamma_0 \Omega_a dp \quad (4)$$

where  $s_a^v$  is the entropy of one atom inside the crystal,  $\Omega_a$  is the atomic volume.

Hence

$$\begin{aligned} \left(\frac{\partial\gamma}{\partial p}\right)_T &= -\Gamma_0 \Omega_a \\ \left(\frac{\partial\gamma}{\partial T}\right)_p &= -\Gamma_0 (s_a^s - s_a^v) = -\frac{q}{T} \end{aligned} \quad (5)$$

where  $q$  is the specific heat of grain boundary formation.

The grain boundary excess free volume can be expressed from (5) as:

$$V_{gb}^{ex} = -\Gamma_0 \Omega_a = \frac{\partial\gamma}{\partial p} \quad (6)$$

It should be pointed out that along with grain boundaries also domain walls and liquid foams possess these thermodynamic properties.

The thermodynamic consideration given above provides a theoretical basis of our experimental approach.

#### Experimental measurements of the grain boundary excess free volume

The proposed method was realized in specially grown tricrystals where the triple junction is formed by two high angle grain boundaries GB1 and GB2 with equal grain boundary surface energy  $\gamma_1 = \gamma_2 = \gamma$  (Fig. 1). The third grain boundary has to be a low angle grain boundary whose surface energy  $\gamma_3$  can be calculated according to the Read and Shockley approach [15]. The system in Fig. 1 is homogeneous through the thickness of the tricrystal, i.e. the triple junction line is rectilinear and runs perpendicular to the plane of diagram. Since through the thickness all three grain boundaries extend perpendicular to the plane of diagram, the configuration of the grain boundary system

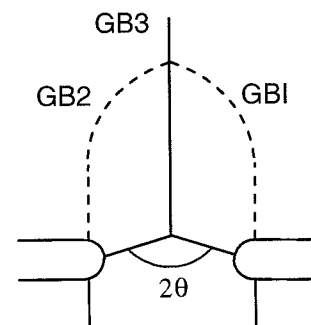


**Fig. 1** Grain boundary geometry to determine the BFV: the grain boundary system with triple junction attains an equilibrium configuration at the notches introduced from the lateral surfaces of the tricrystal

in Fig. 1 is quasi-two-dimensional. So, the motion of the grain boundary system is similar to the motion of a grain boundary system with a triple junction [13], until GB1 and GB2 arrive at the notches (Fig. 1). Boundary motion will cease, and force equilibrium at the triple junction will be established. In this equilibrium the contact angle  $2\theta$  reflects the balance between the energy of boundaries GB1, GB2 and GB3 at the given temperature and pressure

$$2\gamma \cos \theta = \gamma_3 \tag{7}$$

The Eqs. (6) and (7) give us the relationship between the contact angle and the hydrostatic pressure

$$\frac{\partial \gamma}{\partial p} = \frac{2\gamma \frac{\partial \theta}{\partial p} \sin \theta + \frac{\partial \gamma_3}{\partial p}}{2 \cos \theta} \tag{8}$$

In Eq. (8)  $\theta$ ,  $\frac{\partial \theta}{\partial p}$  and  $\gamma$  are experimentally measured quantities. (The grain boundary surface tension  $\gamma$  can be found from (7), if the surface tension of the low angle boundary is measured or calculated.) In our consideration we neglect the influence of the torque terms. To define the derivative  $\left(\frac{\partial \gamma_3}{\partial p}\right)_T$  the following approach was used. According to Read and Shockley [15] a low angle grain boundary can be represented by a periodic arrangement of lattice dislocations. In particular, a low angle twist grain boundary is represented by at least two sets of screw dislocations. The elastic energy of a screw dislocation (apart from the dislocation core energy) is not affected by the hydrostatic pressure, since a screw dislocation represents a state of pure shear. The energy of the dislocation core does not exceed 10% of the total energy of the dislocation. The effect of the hydrostatic pressure on the lattice constant and, therefore, on the dislocation and low angle boundary energy is less than 10%. It can, therefore, be assumed that the energy of a low angle twist grain boundary does not change with an increase of hydrostatic pressure.

If the grain boundary GB3 in Fig. 1 is a low angle twist boundary and  $\left(\frac{\partial \gamma_3}{\partial p}\right)_T \cong 0$ , Eq. 8 can be re-written as

$$\left(\frac{\partial \gamma}{\partial p}\right)_T = \gamma \left(\frac{\partial \theta}{\partial p}\right)_T \cdot \tan \theta \tag{9}$$

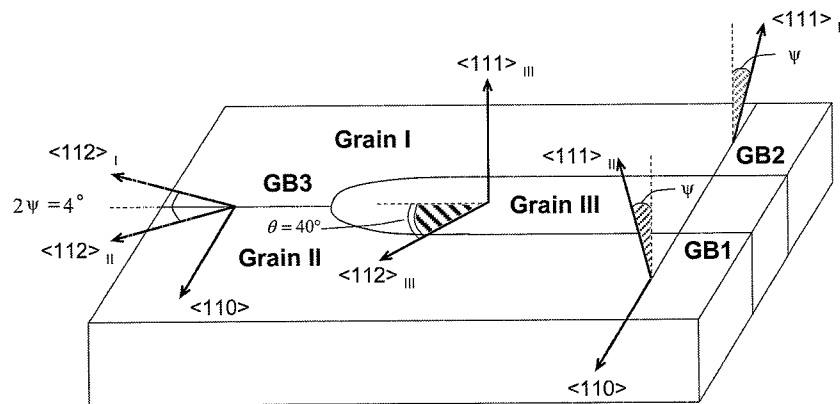
and BFV can be expressed as

$$V_{gb}^{ex} = \gamma_3 \frac{\sin \theta}{2 \cos^2 \theta} \frac{\partial \theta}{\partial p} \tag{10}$$

The experiments were carried out on high purity aluminum (99.999%). Figure 2 shows the geometrical configuration of the investigated tricrystals. The two asymmetrical  $40^\circ \langle 111 \rangle$  tilt grain boundaries (GB1 and GB2) were superimposed by a rotation around the axis perpendicular to the grain boundary plane by an angle  $\psi$  of  $2^\circ$ . The third grain boundary (GB3) was therefore a low angle twist boundary with rotation angle of  $4^\circ$  and the rotation axis  $\langle 110 \rangle$ . Also, the grain boundary system comprised of two  $40^\circ \langle 111 \rangle$  tilt grain boundaries (GB1 and GB2) and an  $80^\circ \langle 111 \rangle$  tilt boundary (GB3) was investigated. The tricrystals were grown from specially oriented seeds in a horizontal Bridgman furnace. The orientation of the crystallographic axes of the crystals was measured by the Laue back-reflection method. The samples were annealed at  $630^\circ\text{C}$  for 60 min under a hydrostatic pressure up to 14 kbar. The temperature of annealing and the pressure were kept constant within  $\pm 1^\circ\text{C}$  and  $\sim \pm 0.1$  kbar, respectively. At the end of annealing the decompression of the experimental cell resulted in a rapid cooling of the sample. Therefore, it can be assumed that the measured value of the contact angle reflects the situation under high pressure.

The center grain of the tricrystal was notched by two straight cuts with an electrical discharge machine in order to arrest the boundary during annealing (Fig. 1). For the measurement of the vertex angles at the triple junctions SEM micrographs of the respective samples

**Fig. 2** Geometry of tricrystals used in experiment



were used (Fig. 3). The crystallographic parameters of the third grain boundary for different samples differed slightly, in the range of  $\pm 0.5^\circ$ . This small deviation does not change perceptibly the properties of high-angle grain boundaries, however, for the energy of the low-angle grain boundary it might be essential. That is why in Fig. 4 the measured pressure dependence of the surface tension  $\gamma$  is presented. (The surface tension  $\gamma$  was determined from Eq. 7 and the Read–Shockley equation for the energy of the low-angle grain boundary [13] for each specific sample.)

Then the value of the BFV for a  $40^\circ\langle 111 \rangle$  tilt grain boundary could be extracted according to Eqs. 6 and (8) and the experimental data presented in Fig. 4. It was found that  $V_{gb}^{ex} = 6.4 \times 10^{-11} \text{ m}^3/\text{m}^2$ . To check the obtained results the pressure dependence of the equi-

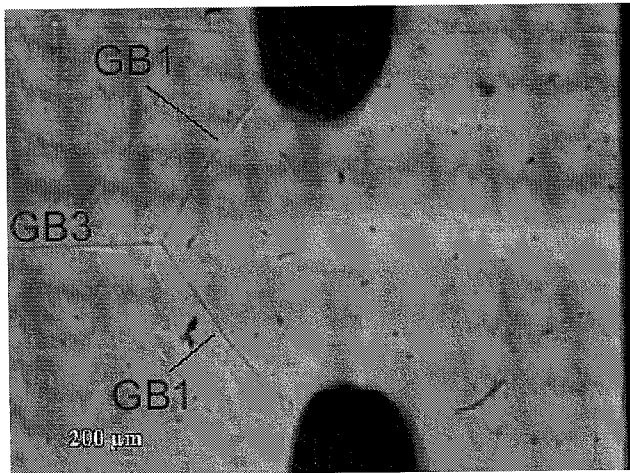


**Fig. 3** SEM image of investigated grain boundary system after annealing

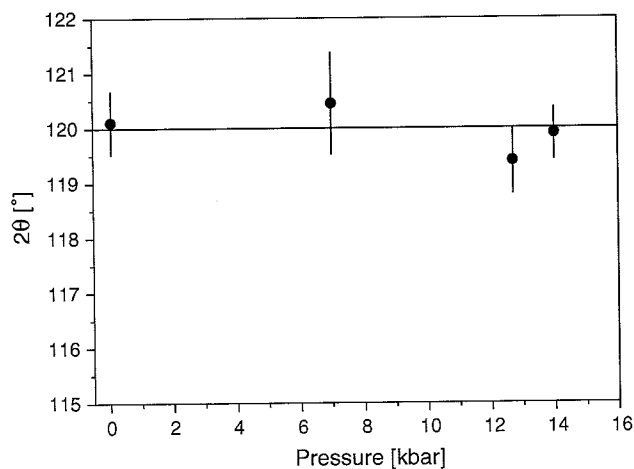


**Fig. 4** Pressure dependence of the equilibrium vertex angle  $2\theta$  for a tricrystal with two  $40^\circ\langle 111 \rangle$  tilt grain boundaries (GB1 and GB2) and an  $80^\circ\langle 111 \rangle$  tilt boundary (GB3)

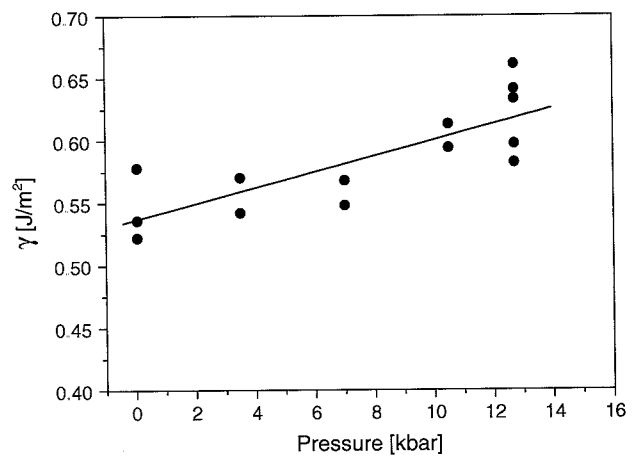


**Fig. 5** Pressure dependence of grain boundary surface tension  $\gamma$  of high-angle boundaries

librium vertex angle  $\theta$  was measured for a grain boundary system of two  $40^\circ\langle 111 \rangle$  tilt grain boundaries as GB1 and GB2 and an  $80^\circ\langle 111 \rangle$  tilt boundary as GB3. Due to crystal symmetry  $80^\circ\langle 111 \rangle$  corresponds to  $-40^\circ\langle 111 \rangle$ , and the grain boundary energy of GB3 should be the same as the energy of GB1 and GB2. The results of the measurements are shown in Fig. 5. The measured angle was about  $120^\circ$  in the whole pressure range and, what is of importance

$$\left(\frac{\partial\theta}{\partial p}\right)_T = 0.$$

It is noted that the quantity  $V_{gb}^{ex} = -\Gamma_0\Omega_a$  defines the absolute value of the BFV, which does not depend on the grain boundary model used, for instance, on the grain boundary width.

The approach put forward opens up new fields of experimental research. In particular, it makes it possible to determine the border between low and high angle boundaries.

**Acknowledgements** Financial assistance from the Deutsche Forschungsgemeinschaft (Grant MO 848/7-1) is gratefully acknowledged. The cooperation was supported by the Deutsche Forschungsgemeinschaft (DFG Grant 436 RUS 113/714/0-1(R)) and the Russian Foundation of Fundamental Research (Grant DFG-RRFI 05-02-04017).

## References

1. Estrin Y, Gottstein G, Shvindlerman LS (1999) Scripta Mater 41:385
2. Estrin Y, Gottstein G, Rabkin E, Shvindlerman LS (2000) Scripta Mater 43:141
3. Estrin Y, Gottstein G, Shvindlerman LS (1999) Acta Mater 47:3541

4. Estrin Y, Gottstein G, Shvindlerman LS (1999) Scripta mater 41:415
5. Knizhnik GS (1981) Poverhnost: Fizika, Khimia, Mehanika 5:50 [In Russian]
6. Wolf D (1989) Scripta Metall 23:1913
7. Wolf D (1990) Acta Metall 38:781
8. Frost HJ, Ashby MF, Spaepen F (1980) Scripta Metall 14:1051
9. Stremel MA, Markovich AL (1997) Poverhnost 1:85 [In Russian]
10. Zhang H, Srolovitz DJ. To be published
11. Meiser H, Gleitter H (1980) Scripta Metall 14:1980
12. Merkle KL, Csencsits R, Rynes KL, Withrow JP, Stadelmann PA (1998) Journal of Microscopy 190:204
13. Gottstein G, Shvindlerman LS (1999) Grain Boundary Migration in Metals: Thermodynamics, Kinetics, Applications. CRC Press, Baton Rouge
14. Fradkov V, Shvindlerman LS (1979) Fiz Metall Metalloved 48:297
15. Read WT, Shockley W (1950) Phys Rev 28:275